Jeffery Nathan (Orcid ID: 0000-0001-5166-2029)

A human craniofacial life-course: cross-sectional morphological covariations during postnatal growth, adolescence, and aging

Running title: Cranial & brain covariation

Nathan S. Jeffery, Craig Humphreys & Amy Manson

Human Anatomy Resource Centre & Institute of Life Course and Medical Sciences, University of Liverpool, Liverpool, UK.

Corresponding author: Nathan Jeffery (njeffery@liverpool.ac.uk), Human Anatomy Resource Centre, Sherrington Bld., Ashton St., Liverpool, L69 3GE

Data Availability

All image data are available via the repositories listed within the acknowledgements and Table 1.

Ethics & consents

All image data were originally collected with ethical permissions and consent. Please refer to the individual repositories for further details.

ORCID
Nathan Jeffery https://orcid.org/0000-0001-5166-2029
Amy Manson https://orcid.org/0000-0001-6879-3551
Craig Humphreys: https://orcid.org/0000-0002-5866-979X

Keywords: Spatial-packing, brain, cranium, ontogeny, aging, sexual dimorphism

Abstract

Covariations between anatomical structures are fundamental to craniofacial ontogeny, maturation and aging and yet are rarely studied in such a cognate fashion. Here we offer a comprehensive investigation of the human craniofacial complex using freely available software and MRI datasets representing 575 individuals from 0 to 79 years old. We employ both standard craniometrics methods as well as Procrustes based analyses to capture and document cross-sectional trends. Findings suggest that anatomical structures behave primarily as modules, and manifest integrated patterns of shape change as they compete for space, particularly with relative expansions of the brain during early postnatal life and of the face during puberty. Sexual dimorphism was detected in infancy and intensified during adolescence with gender differences in the magnitude and pattern of morphological covariation as well as of aging. These findings partly support the spatial-packing hypothesis and reveal important insights into phenotypic adjustments to deep-rooted, and presumably genetically defined, trajectories of morphological size and shape change that characterize the normal human craniofacial life-course.

1. Introduction

Allometric shifts of brain size can unleash a network of physical interactions that constrain and integrate the form (size & shape) of neighbouring structures of the cranium (see review in Lesciotto & Richtsmeier, 2019; Jeffery et al, 2021). The effect is considered a particularly potent agent for changes of the human basicranium and face as the cranium accommodated a four-fold increase of brain size during the last few million years of hominin evolution (McHenry, 1994) and many times that again during each successive ontogeny (Dobbing & Sands, 1973). The bulk of this ontogenetic encephalization has shifted postpartum in humans, most likely in response to limitations imposed by the size of the birth canal (see Rosenberg & Trevathan, 2002; DeSilva & Rosenberg, 2017). Less than 50% of brain growth occurs postpartum in extant cercopithecids, increasing to around 60% in extant *Pan troglodytes,* as well as extinct early australopithecines, and rising further to 70% in *Homo sapiens* (see DeSilva & Lesnik, 2008). Here we investigate cranial form changes associated with this 70% of human encephalization that occurs postnatally, as well as culminating intraspecific covariations amongst adults, including sexual dimorphism. A correlate of encephalization in humans, and other primates, is extended life expectancy (Harvey & Clutton-Brock, 1985). Prolonged somatic senescence is in turn associated with phenotypic instability, reflecting cellular and physiological deterioration, and the greater timeframe over which intraspecific life-histories can diverge and their differential effects can manifest. We therefore also consider here the life-course throughout adulthood, including morphological variations possibly linked to the prolonged human craniofacial senescence.

Whether the skull, and parts thereof, seemingly covary with the brain (integration) or vary as independent units (modularity) partly depends on the morphologies, species, and age ranges studied. Integration is not an invariant property. It tends to vacillate over time, across different length scales as well as between anatomical regions, individuals and species according to differences of phylogeny, development, function and architectural conformity (see Goswami, 2006; Zollikofer et al, 2017; Mitteroecker & Bookstein 2008; Jeffery et al., 2021). Hence, patterns of covariation can be hard to define, let alone decipher, within the aggregate of many such trends, staggered and superimposed over one another as in Hallgrímsson et al's (2009) Palimpsest analogy. One approach often favoured in macroevolutionary studies is to conceptually and statistically render interpretations from the resulting medley on the assumption that the aggregate is generally representative and mostly summative rather than compensatory in nature. Another approach is to hone the study design to minimize the number of trends examined and iteratively test for specific sources of covariation. Here we take the latter approach, focusing on humans and the proposed role of relative brain enlargement in shaping variations of the underlying cranial base and face – otherwise known as the spatial-packing hypothesis (see Ross & Ravosa, 1993; Jeffery et al, 2021; Lesciotto & Richtsmeier, 2019). This predicts that fluctuations of brain size relative to that of the skull, typically basicranial size, correlate with changes of basicranial and facial form, most commonly represented by cranial base angle (CBA) and the angle of facial kyphosis

(AFK). More specifically, increases of relative brain size are associated with cranial base flexion (↓CBA) and facial kyphosis (↓AFK) whereas decreases, in which regions of the skull scale with positive allometry against brain size, are associated with cranial base flattening, also referred to as retroflexion (↑CBA) and dorsal deflection of the face (↑AFK). We test for these predicted changes on the basis of standard craniometrics such as CBA and AFK as well as of Procrustes based geometric morphometrics using data obtained from MRI scans representing 575 individuals aged 0 to 79 years. Below we briefly review the existing literature on ontogenetic and adult intraspecific covariations of the modern human cranium and brain.

1.1 Ontogeny

There are numerous ontogenetic studies that encompass the human brain as well as the basicranium and several of these document correlative phases of cranial base and facial angulation with brain growth (e.g. Lieberman & McCarthy, 1999; Neubauer et al., 2009; Zollikofer et al., 2017). However, not all observations are consistent with the spatial-packing hypothesis. For example, during fetal life CBA and equivalent measures for AFK appear to increase whilst the brain enlarges substantively, both in absolute and relative terms (e.g. Jeffery and Spoor 2002, 2004; Jeffery, 2003). This is preceded by concomitant flexure of the brain, the pharyngeal region and the cartilaginous basicranium, which is linked to formation of the secondary vesicles during embryogenesis (e.g. Diewert, 1983; Dambricourt-Malassé, 1993). After birth, CBA decreases again by around 10 degrees with most of the flexion occurring in the first postnatal year (e.g. Lieberman and McCarthy 1999) and accompanied by a period of rapid brain growth (e.g. Jin et al. 2014) as well as downward displacement of the face (e.g. Enlow, 1968). Brain growth is considered the principal determinant of skull architecture at this time and several studies report findings that are consistent with brain related spatial-packing (e.g. Zollikofer et al. 2017). By the second postnatal year over 90% of adult brain size is achieved (Dobbing & Sands, 1973) whilst many parts of the skull continue to grow and change for at least another decade (e.g. Bastir, et al 2006; Neubauer et al., 2009). As the dominance of brain growth wanes, the influences of new or other previously obscured sources of covariation gradually emerge. Most notable of these are reported covariations of the cranial base with the face (e.g. Bastir & Rosas, 2006). In summary, the above studies suggest that spatial-packing related changes of cranial base and facial form are correlated with increases of absolute and relative brain size during the first year of postnatal life, but then these correlations diminish thereafter and associations directly between the face and cranial base become more prominent. We test these predictions for the first time with data representing a large sample of 575 individuals, spanning the whole of postnatal ontogeny.

1.2 Adulthood

The most prominent morphological trend seen amongst healthy adults is that of sexual dimorphism. Relative to females, modern human males are on average 12% larger in

terms of body size (Smith & Cheverud, 2002) and this scale difference, as well as its allometric effects, are also manifested in the brain and skull. Previous studies suggest relative to adult females, adult male cerebri are around 9% larger by volume (Giedd et al., 1997) and their skulls are some 11% larger as well (Gonzalez et al., 2011). Researchers have also noted differences of skull shape. These include marked differences of the mandible and of muscle attachments, and that females tend to have relatively smaller naso- and oro-pharyngeal spaces associated with a flatter basicranium in comparison with males (Rosas & Bastir, 2002). Earlier work suggests that sexual dimorphism of the anterior cranial base is established during childhood whilst that of the face emerges later, around puberty (Ursi et al, 1993). More recently, Smith et al's (2020) analyses of surface landmarks has suggested that craniofacial sexual dimorphism is mostly size related and that males follow an extended growth trajectory (hypermorphosis). This size offset has also been confirmed in a recent study of skeletal landmarks (Milella et al., 2021) with males, on average, more prognathic and dolichocephalic compared with females. In the present study we test for sexual dimorphism in the size and shape of the brain as well as of the cranium across a large population, including during ontogeny and adulthood.

Another trend seen later in adulthood is senescence. Humans have one of the highest longevity quotients (Sacher, 1959) and our extended lifespan is considered a group selective advantage (Alvarez, 2000). The effects of extended senescence and assumed morphological decline on covariations has yet to be investigated. Some evidence suggests the skull responds to age-related events like shifts of hormonal regulation amongst females, behavioural changes such as adopting a more sedentary lifestyle, deteriorating dental health, and tooth loss (see Albert et al., 2007). Commonly reported morphological changes include the relative proportions and position of the midface as well as skull enlargement and increased calvarial thickness (Israel, 1973; Pecora et al., 2006; Mendelson & Wong , 2012; Levine et al, 2003; Levine, 2008; Bartlett et al., 1992; Albert et al., 2007; Farkas et al. 2013; Doual et al., 1997). Brain size reportedly shrinks by around 14% (cerebral volume) from middle to old age with some regions affected more than others (Jernigan et al., 2001), leading to changes of brain shape as well as size. Here, we re-evaluate this evidence base whilst controlling for differences of dentition and including data on the brain and cranium sampled from the same population. We test for cranial enlargement, endocranial shrinkage, representing brain size, and associated shape changes among older adults as well as for gender differences of aging. We also test the proposition that that older crania will have accumulated more variance due to diverging life experiences as well as fragility and therefore morphological covariations will be weaker in the oldest adults.

2. Material & Methods

Magnetic resonance image datasets were drawn from several open-access repositories, representing *in-vivo* studies of control subjects ranging from birth to 79 years of age (see Table 1). Please refer to the individual study reports for details regarding ethical approvals and consents. Adult datasets were further screened to remove edentulous and partially dentulous subjects (two or more adjacent teeth missing, excluding M3). A total of 575 subjects were included in the current cross-sectional analysis and were subdivided (cut_number function in R v3.6.2) into 10 chronological age bins containing between 56-59 subjects each (see Table 2).

Endocranial volumes were collected from T2 weighted images using the Volumest plugin (v20101017) for ImageJ (v1.50), which is based on the Cavalieri principle (Roberts et al, 2000). Volumes were available for the PING sample (see Table 1; Jernigan et al., 2016). Three-dimensional co-ordinates for 23 cranial landmarks were taken from T1 weighted images (see Figure 1) using the mark-up tool in 3Dslicer v. 4.8.1 (Fedorov et al., 2012). A further 17 landmarks were collected to represent the subcortex and basal most parts of the cerebral cortex in close spatial proximity to the cranial base and face. Both configurations were chosen to provide reasonable morphological representation as well as fidelity (predominantly type I & II landmarks) whilst also ensuring sample sizes were close to, or exceeded, Procrustes space dimensionality and avoiding outlier landmarks that can leverage Procrustes fitting (see Bookstein, 2017 and Cardini, 2019). Craniometric measures derived from the landmarks included centroid sizes (sum of the squared inter-landmark distances) for the whole cranium, the brain, the basicranium and the face. Measurements of Cranial Base Angle (CBA) and the Angle of Facial Kyphosis (AFK) were also derived from landmark sets (see Table 3) using trigonometry. Indices of relative encephalization IREb, IREf and IREc were computed using cube root endocranial volume (ECI) as the numerator and basicranial, facial and whole cranium centroid sizes as the denominator, respectively. We selected these denominators over, for example, basicranial length because the lateral cranial base is equally as important as the midline in accommodating the brain. All data were collected by authors CH and AM. Both intra- and inter-observer landmarking was checked and found to be comparable as well as repeatable (between subjects and repeats ANOVA mean square centroid sizes were 5194 and 6, respectively [$p<0.001$]). Measurements and landmarks are summarized in Table 3. Statistical analyses of craniometric data were conducted in R (v3.6.2).

Landmark configurations were subjected to Procrustes based geometric morphometric form analyses using MorphoJ v1.07a (Klingenberg, 2011). Three-dimensional Procrustes fits (combined and separate) with object symmetry were used to extract the symmetric component of the Procrustes space. Covariates included age (years), cranial centroid size, and the indices of encephalization (IREb, IREf & IREc). Classifiers included gender and age bins. Trends within the Procrustes space were explored using multivariate regression. Residuals from regressions against whole cranium centroid size were used to limit the effects of size and explore non-allometric shape changes. Note, we use the

terms allometric and non-allometric throughout to refer to analyses with the uncorrected Procrustes data and that conducted with residuals from cranial centroid size regressions. Other tests conducted in MorphoJ included discriminant functions between genders and age bins. Tests of integration between the cranium and brain (brain-cranium) as well as between the basicranium and face (face-base) landmark partitions were calculated in MorphoJ using RV coefficients from within configuration Partial Least Squares (PLS) analyses and Modularity tests based on a full Delaunay triangulation representation of spatial contiguity (see Klingenberg, 2009 and 2011). The RV metric has been subject to criticism of late (Adams, 2016; Adams & Collyer, 2019) so we also tested for modularity by calculating the covariance ratio (CR) coefficient and modularity effect size (Z_{CR}) in the R (v3.6.2) package *geomorph* (v3.3.2) using the symmetric components exported from MorphoJ. A CR coefficient less than 1 is indicative of modularity and Z_{CR} approximates the relative strength of modularity between alternative scenarios, in our case brain-cranium and face-base (see above and worked examples in Adams & Collyer, 2019).

3. Results

3.1 Craniometrics

Bivariate comparisons against age are shown in Figure 2. These suggest that endocranium size increased rapidly during the first few years of life. By contrast, the cranium, represented by overall (CS), base (Bcs) and face (Fcs) centroid sizes, grew at a slower rate but over a longer 18year period. Within the cranium, the face grew for longer and initially slower than the base. This was also revealed by the upward then downward trend for the index of basicranial over facial centroid size (Bfi). Indices of relative encephalization decreased during the first two decades of life. Patterns for angles were less clear. There was a small decrease of CBA earlier in postnatal life. The overall Spearman correlation matrix revealed significant associations between most variables including those that support the spatial packing hypothesis (Figure 3a). The strongest negative associations were between centroid sizes and encephalization indices, reflecting increases of the denominator variables. The strongest positive correlations were among cranium size variables. Values of AFK positively covaried with size as well as age and negatively covaried with all three indices. CBA showed a smaller negative correlation with endocranial volume, Bfi, and IREf, suggesting the face is an important factor.

The above observations were confirmed by Wilcoxon tests between adjacent age bin (Figure 4) and Spearman correlation matrices (Figure 3b). Ranges and sample sizes for each bin are given in Table 2. These plots and correlation matrices suggest that endocranial volume increased significantly from birth until around 3 years of age. Centroid sizes consistently increased with age from birth until adulthood. CBA and AFK showed weak decreases during the first year (Figure 3b) with possible upward shifts later in life. In particular, AFK showed an increase from around 2 to 5yrs with a possible decrease

later in adulthood (Figure 4). Bfi and IREf increased during the first year (Figure 2) and then decreased later in ontogeny (Figure 3b). IREb and IREc decreased throughout ontogeny from birth. These findings highlight covariations of infant cranial base flexion, facial kyphosis (ventral deflection) and relative enlargement of the endocranium (IREf) and changes in the proportions of the face and cranial base (Bfi). There was also limited evidence for a subsequent, pubescent, period of negative correlation between AFK and relative endocranial size (see Figure 3b). These findings are broadly consistent with an initial phase of spatial-packing between the brain and face followed by a later phase of spatial-packing between the face and basicranium.

Wilcoxon tests between female and male means are shown in Table 4 for bins containing more than 20 individuals per gender (see Table 2). Findings revealed size dependent sexual dimorphism from infancy (5.17-10.6yrs) with males larger on average than females. Interestingly, the face size (Fcs) was last to emerge as size dimorphic. There was also limited evidence for sporadic dimorphism of the encephalization indices, apart from IREf. There was no significant difference of AFK or CBA between males and females (Table 2). However, adult males appeared to experience subtly stronger covariations involving AFK and size (Figure 5) and of aging (Figure 6). The oldest adult males (47-79yrs) had, on average, slightly more kyphotic faces than the middle aged adult males (27-47yrs) whereas the oldest females had slightly larger crania compared with the middle aged adult females, though this was on the cusp of the $p>0.05$ threshold. In conclusion, the craniometric analyses produced results that were indicative of spatial-packing in neonates, sexual dimorphism from infancy, and of subtle divergent trends of craniofacial aging.

3.2 Procrustes Analyses

Regressions of the symmetric component of the cranium shape revealed that cranial centroid size and age predict around 25% and 19% of the total allometric shape variation, respectively (see Table 5). Indices of relative encephalization also predicted significant and substantive percentages of the allometric shape variation across all subjects, all males, and all females (14 to 27%). Across Bins 1 and 2, age predicted the most variation closely followed by those indices involving the face (Bfi & IREf). In keeping with the craniometrics, Bfi consistently predicted the most shape variation across the remaining age bins. There was little evidence for substantive non-allometric shape covariations. Figure 7a-b illustrates the allometric shape variations associated with age and Bfi during the first 18months of life. These revealed flexion of the anterior and posterior cranial base, ocular convergence as well as slight facial kyphosis. Trends were most prominent in relation to Bfi and were similar for the other indices investigated. Figure 7c illustrates the weak (2%; $p=0.0181$) shape variation predicted across adulthood. It shows slight facial kyphosis and ventral depression of the eyes. There was no discernible difference of distribution between males and females, nor of data variability between middle aged adults and the older adults.

Results for discriminant functions between adjacent age bins are shown in Table 6 for allometric and non-allometric (size corrected residuals) data. These confirmed that the period of greatest form change, as measured by Procrustes distance, was during the first few years of postnatal life (bins 1-2). Differences of form included cranial base flexion, mostly of the posterior cranial base, as well as ocular convergence (Figure 8a). These trends remained after size correction (Table 6). Females showed a modest difference compared with males and vectors differed by 16 degrees for separate gender regressions against centroid size ($p<0.00001$). Figure 8d summarizes the allometric differences between males and females. Males tended to have longer posterior cranial fossae, more flexed posterior basicrania and slightly more kyphotic faces. These findings indicated that males and females have slightly different forms and perhaps follow different trajectories as well.

Discrimination between age bins was also detected later in life, including childhood as well as adulthood. Functions between bins 5 and 6 revealed ventral deflection of the anterior cranial base and face (Figure 8b). Aging effects (bins 9 and 10) were not detected within separate fits for males and females, probably due to the smaller sample sizes (females [n=29,32], PD 0.0179; p-value = 0.133; Males [n=28,26], PD 0.0188; p = 0.237). The mixed sex discriminant function (n=57,58) was significant, though weak and spanned a slightly shorter Procrustes distance (see Table 6). The oldest mixed gender individuals tended to have slight dorsal elevation at the back of the face, consistent with reduced AFK, as well as anterior rotation of the eyes and posterior displacement of the posterior cranial fossa (Figure 8c). These analytical steps were repeated for the brain landmarks.

Discriminant functions (Table 6) for the brain landmarks revealed similar ontogenetic phases of allometric and non-allometric shape change with notable shifts during the first year (bins 1-2) and another larger shift from around 5 to 17yrs (bins 6-7). Procrustes distances are in general larger than those seen for the cranium. Significant changes of form continued through puberty and into adulthood. Form differences are illustrated in Figure 9. During the first year, there were relative expansion of the cerebrum posteriorly and contraction anteriorly and dorsoventrally. From bins 6 to 7 the pons enlarges slightly, and the frontal poles decrease in relative size. In old age (bins 9-10), the posterior cerebrum and internal capsule seemingly enlarge relative to the anterior cerebrum, which remained relatively unaffected by aging. Discriminations between bins 9 and 10 were slightly stronger in males (PD 0.04546522; p=<.0001; [n=27,25]) compared with females (PD 0.03915803; p=<.0001; [n=29,33]) despite the small sample sizes. Across age groups there was moderate discrimination between males and females (Table 6). Findings for the non-allometric shape variation were similar.

Landmark sets were subsequently tested for morphological integration between the brain-cranium and face-base (see Table 7). The Partial Least Squares (PLS) within configuration analysis yielded an overall RV coefficient of 0.71 (p=<.001) for brain-cranium. Analysis across genders and age bins (separate fits) suggested that there was brain-cranium integration in males, females as well as adolescents (bins 6-7) and possibly

among neonates (bins 1-2). Klingenberg modularity tests further supported the notion of brain-cranium integration for males and young adults. Among both groups, outward displacement of the brain landmarks was associated with cranial base flexion and facial kyphosis. With one exception the covariance ratio coefficients were less than 1. This suggested a general trend of modularity, especially amongst females and children 1 to 5years. There was little evidence for closer integration of the face-base compared with that of the brain-cranium. Indeed, among neonates, for example, and across bins 6 to 8 the modularity effect (Z_{CR}) was slightly greater for the face-base scenario. The biggest difference (Δ1.39) of Z_{CR} was for Bins 1&2, suggesting that face-base units vary in a more modular fashion compared with brain-cranium units among neonates. There was no evidence to suggest that older adults exhibited more or less modularity.

Discussion

We confirm that the first year of postnatal life is the period of greatest morphological change, and of significant covariation between the cranium, including cranial base flexion and facial kyphosis, and relative brain size. These data partly support the spatial-packing hypothesis and corroborate findings reported by, for example, Lieberman and McCarthy (1999), Neubauer et al (2009) and Zollikofer et al. (2017). Furthermore, our investigation showed that competition for space between the face and the brain was the strongest correlate and suggests that growth of the face is a significant contributory factor for much of ontogeny, perhaps becoming the principal factor during adolescence. This supports previous studies by Bastir and others (Bastir & Rosas, 2006; Bastir et al 2010; Neubauer et al., 2009; Zollikofer et al., 2017). It seems likely that several other, if not all, morphological units play a part in spatial-packing like phenomena during ontogeny but that we tend to see their individual and combined effects at different time points and to varying degrees, either because they have indeed strengthened and/or because the effects of other units have abated. In other words, we have a problem of entangled ontogenetic covariations of which we only ever see the averaged phenotypic outcome. Other contributory factors to consider in this mix include, for example, growth of the eyes, nasal septum and masticatory muscles (e.g. Jeffery et al., 2007; Jeffery et al., 2021) as well ontogenetic shifts of basicranial compliance and growth potential linked to patency of the synchondroses (see Hoyte, 1973; Thilander and Ingersal, 1973; Jeffery & Spoor, 2002; Smith et al., 2021b). Recent work has demonstrated how computational growth simulations can potentially tease apart some of these entwined effects (e.g. Jeffery et al 2021).

The neonatal period of covariation was accompanied by rapid brain growth. We found most of brain growth was completed, on average, by 3yrs of age, which is consistent with results reported by, for example, Guihard-Costa & Ramirez-Rozzi (2004). By contrast, the face and basicranium continued to grow for much longer, albeit at slower rates, up to and into early adulthood. Changes in the index of base over face size suggest that base growth is faster than the face initially (↑Bfi) but is overtaken by that of the face (↓Bfi) later

in childhood and adolescence. The disparity in the rate and eventual maturation of different parts of the cranium is consistent with previous findings (e.g. Bastir, et al 2006; Neubauer et al., 2009). Interestingly, brain shape as defined here continues to change beyond 3yrs, with the greatest shift occurring from 5 to 17yrs. This may mirror the closer proximity of our brain landmarks to the slower growing skull base, or the later maturation of, for example, associative cortices and the necessary adjustments of their anatomical correlates within the same volumetric confines. There is significant grey matter sculpting and synaptic pruning during this period of adolescence (e.g. Whitford et al., 2007). For example, Sowell et al. (2001) report that such modifications are particularly prominent within the frontal region, which showed a relative reduction of size from 5 to 17yrs in our study.

Whilst covariations of craniometrics and Procrustes based morphometrics with indices were moderate, the formal tests for integration between shapes defined by landmark configurations revealed only weak effects. The peak signals for integration were among males and adolescents, and only then between the brain and the cranium. Otherwise, it seemed that shape variations were manifested largely via independent modules representing the face, basicranium and brain. The apparent discrepancy with respect to the indices may partly reflect the choice of brain landmarks, which excluded the potentially deleterious leveraging effects of points distal most to the skull base and face, along the dorsal surface of the cerebrum. However, it is also important to note that these two sets of findings are not mutually exclusive. The evidence for modularity only suggests that correlations within modules were stronger, representing the co-ordination of shape according to, for example, tissue type and developmental process, than the overlying spatial integration detected by comparisons against the indices. These findings illustrate the importance of a nuanced interpretation of such powerful techniques as opposed to dichotomising complex, multi-layered, systems as either integrated or modular.

That there were signals suggesting shape integration amongst older-children, adolescents, and males could well herald the emergence of sexual dimorphism. Gender differences of size were established well before puberty and our study suggests that males experienced subtly different patterns of brain and of cranial aging as well as growth. These findings are consistent with recent work published by Smith et al. (2020 & 2021a) as well as Milella et al. (2021). We find no evidence that the aged adult cranium is more variable due to, for example, fragility nor that covariations were any weaker or stronger compared with middle aged adults. We avoid drawing conclusions here based on comparisons with younger adults (<27yrs) as they were likely to differ due to partial osteological maturation. Our findings suggest that aging is more marked, or at least more readily measured among males. This was somewhat surprising given the proposed systemic and widespread effects of the menopause on aging in females and previous work (Windhager et al., 2019) but is consistent with other recent studies (e.g. Smith et al 2021a). In the latter study the authors report stronger associations between soft-tissue facial form and age in older males than in older females. In our sample, older males tended to have slightly more kyphotic faces when measured using craniometrics and

Procrustes based morphometrics. In terms of shape, older brains (mixed gender) tended to be relatively expanded and a little flexed posteriorly. Again, the brain aging effect seemed stronger in males. We did not, however, detect any age-related differences of endocranial volume. Caution is warranted regarding the single sex discriminant functions between adults and aged adults. The sample sizes were much smaller (n<33), and closer to the dimensionality of the shape space (see Bookstein, 2017 and Cardini, 2019). We must also be wary of overinterpreting all such trends based on cross-sectional data. Nonetheless, overall the present study sheds considerable light on important trends and patterns of covariations that help us better understand the life-course of the craniofacial complex from the cradle to the grave, appreciate the rippling of multifactorial influences through the physical connections of the head and will no doubt help inform future clinical, experimental and computational studies.

Conclusions

We find that the first few years of postnatal life are indeed the most morphologically active with steep growth trajectories and covariations of the cranium with relative size of the brain and particularly of the face. These findings partly support the spatial-packing hypothesis. Our study may also have captured the anatomical correlates of brain maturation, especially of the frontal cortex, during adolescence as well as the morphological divergence of the brain and of the cranium between males and females, and the acceleration of sexual dimorphism during puberty and thereafter. The present study also highlighted aging of the craniofacial complex, finding more prominent, or at least readily measurable, age effects amongst males. Overall, it appeared that anatomical structures of the head operate principally as modules and that integrated covariations emerge as these modules compete for space whilst maintaining functional integrity and structural conformity.

Acknowledgements

Firstly, would like to thank and acknowledge the data repositories:

Information eXtraction from Images (IXI) project – Data were made available under creative commons license (CC BY-SA 3.0) via https://brain-development.org/ixi-dataset/

National Database for Autism Research (NDAR) - Data and/or research tools used in the preparation of this manuscript were obtained from the NIH supported National Database for Autism Research (NDAR). NDAR is a collaborative informatics system created by the National Institutes of Health to provide a national resource to support and

accelerate research in autism. Dataset identifier(s): DOI: 10.15154/1520729. This manuscript reflects the views of the authors and may not reflect the opinions or views of the NIH or of the Submitters submitting original data to NDAR.

We would also like to thank the developers involved in creating and maintaining R (www.r-project.org), GeoMorph (https://github.com/geomorphR/geomorph), 3Dslicer (www.slicer.org) as well as MorphoJ (www.morphometrics.uk) and ImageJ (imagej.nih.gov). This work was not funded and would not have been viable without their support. Finally, we thank the two anonymous referees for the helpful comments and suggestions.

References:

Adams, D. C. (2016). Evaluating modularity in morphometric data: challenges with the RV coefficient and a new test measure. Methods in Ecology and Evolution, 7(5), 565-572.

Adams, D. C., & Collyer, M. L. (2019). Comparing the strength of modular signal, and evaluating alternative modular hypotheses, using covariance ratio effect sizes with morphometric data. Evolution, 73(12), 2352-2367.

Albert, A. M., Ricanek Jr, K., & Patterson, E. (2007). A review of the literature on the aging adult skull and face: Implications for forensic science research and applications. *Forensic science international*, *172*(1), 1-9.

Alvarez, H. P. (2000). Grandmother hypothesis and primate life histories. *American Journal of Physical Anthropology: The Official Publication of the American Association of Physical Anthropologists*, *113*(3), 435-450.

Bartlett, S. P., Grossman, R., & Whitaker, L. A. (1992). Age-related changes of the craniofacial skeleton: an anthropometric and histologic analysis. Plastic and reconstructive surgery, 90(4), 592-600.

Bastir, M., & Rosas, A. (2006). Correlated variation between the lateral basicranium and the face: a geometric morphometric study in different human groups. *Archives of Oral Biology*, *51*(9), 814-824.

Bastir, M., Rosas, A., Stringer, C., Cuétara, J. M., Kruszynski, R., Weber, G. W., ... & Ravosa, M. J. (2010). Effects of brain and facial size on basicranial form in human and primate evolution. *Journal of Human Evolution*, *58*(5), 424-431.

Bookstein, F. L. (2017). A newly noticed formula enforces fundamental limits on geometric morphometric analyses. *Evolutionary Biology, 44*(4), 522–541.

Bulygina, E., Mitteroecker, P., & Aiello, L. (2006). Ontogeny of facial dimorphism and patterns of individual development within one human population. *American Journal of Physical Anthropology*, *131*(3), 432-443.

Cardini, A. (2019). Integration and modularity in Procrustes shape data: is there a risk of spurious results?. *Evolutionary Biology*, *46*(1), 90-105.

Dambricourt-Malassé, A. (1993). Continuity and discontinuity during hominization. Quaternary International, 19, 85-98.

DeSilva, J. M., & Lesnik, J. J. (2008). Brain size at birth throughout human evolution: a new method for estimating neonatal brain size in hominins. *Journal of human evolution*, *55*(6), 1064-1074.

Diewert, V. M. (1983). A morphometric analysis of craniofacial growth and changes in spatial relations during secondary palatal development in human embryos and fetuses. American journal of anatomy, 167(4), 495-522.

DeSilva, J, Rosenberg, K. (2017). Anatomy, development, and function of the human pelvis. Anatomical Record 300:628–632.

Dobbing, J., & Sands, J. (1973). Quantitative growth and development of human brain. Archives of disease in childhood, 48(10), 757-767.

Doual, J. M., Ferri, J., & Laude, M. (1997). The influence of senescence on craniofacial and cervical morphology in humans. *Surgical and Radiologic Anatomy*, *19*(3), 175-183.

Enlow, D. H. (1968). The human face. An account of the postnatal growth and development of the craniofacial skeleton.

Evans, A.C. 2006. “The NIH MRI study of normal brain development.” NeuroImage, 30(1), pp.184-202.

Farkas, J. P., Pessa, J. E., Hubbard, B., & Rohrich, R. J. (2013). The science and theory behind facial aging. Plastic and Reconstructive Surgery Global Open, 1(1).

Fedorov, A., Beichel, R., Kalpathy-Cramer, J., Finet, J. et al (2012). 3D Slicer as an image computing platform for the Quantitative Imaging Network. *Magnetic resonance imaging*, *30*(9), 1323-1341.

Giedd, J. N., Castellanos, F. X., Rajapakse, J. C., Vaituzis, A. C., & Rapoport, J. L. (1997). Sexual dimorphism of the developing human brain. *Progress in Neuro-Psychopharmacology and Biological Psychiatry*, *21*(8), 1185-1201.

Gonzalez, P. N., Bernal, V., & Perez, S. I. (2011). Analysis of sexual dimorphism of craniofacial traits using geometric morphometric techniques. *International Journal of Osteoarchaeology*, *21*(1), 82-91.

Goswami, A. (2006). Cranial modularity shifts during mammalian evolution. The American Naturalist, 168(2), 270-280.

Guihard-Costa, A. M., & Ramirez-Rozzi, F. (2004). Growth of the human brain and skull slows down at about 2.5 years old. Comptes Rendus Palevol, 3(5), 397-402.

Hallgrímsson, B., Jamniczky, H., Young, N. M., Rolian, C., Parsons, T. E., Boughner, J. C., & Marcucio, R. S. (2009). Deciphering the palimpsest: studying the relationship between morphological integration and phenotypic covariation. *Evolutionary biology*, *36*(4), 355-376.

Harvey, P. H., & Clutton-Brock, T. H. (1985). Life history variation in primates. *Evolution*, *39*(3), 559-581.

Hoyte, D. A. N. (1973). Basicranial elongation: 2. Is there differential growth within a synchondrosis? The Anatomical Record, 175, 347.

Isreal, H. (1973). Recent knowledge concerning craniofacial aging. The Angle Orthodontist, 43(2), 176-184.

Jeffery, N. (2003). Brain expansion and comparative prenatal ontogeny of the non-hominoid primate cranial base. Journal of human evolution, 45(4), 263-284.

Jeffery, N., & Spoor, F. (2002). Brain size and the human cranial base: a prenatal perspective. American Journal of Physical Anthropology: The Official Publication of the American Association of Physical Anthropologists, 118(4), 324-340.

Jeffery, N., & Spoor, F. (2004). Ossification and midline shape changes of the human fetal cranial base. American Journal of Physical Anthropology, 123(1), 78-90.

Jeffery, N., Davies, K., Köckenberger, W., & Williams, S. (2007). Craniofacial growth in fetal Tarsius bancanus: brains, eyes and nasal septa. Journal of anatomy, 210(6), 703-722.

Jeffery, N.S., Sarver, D.C. and Mendias, C.L. (2021), Ontogenetic and in silico models of spatial-packing in the hypermuscular mouse skull. Journal of Anatomy, 238(6), 1284-1295

Jernigan, T. L., Archibald, S. L., Fennema-Notestine, C., Gamst, A. C., Stout, J. C., Bonner, J., & Hesselink, J. R. (2001). Effects of age on tissues and regions of the cerebrum and cerebellum. *Neurobiology of aging*, *22*(4), 581-594.

Jernigan, T. L., Brown, T. T., Hagler Jr, D. J., Akshoomoff, N., Bartsch, H., Newman, E., ... & Dale, A. M. (2016). The pediatric imaging, neurocognition, and genetics (PING) data repository. Neuroimage, 124, 1149-1154.

Jin, J., Shahbazi, S., Lloyd, J., Fels, S., De Ribaupierre, S., & Eagleson, R. (2014). Hybrid simulation of brain–skull growth. Simulation, 90(1), 3-10.

Klingenberg, C. P. (2009). Morphometric integration and modularity in configurations of landmarks: tools for evaluating a priori hypotheses. *Evolution & development*, *11*(4), 405-421.

Klingenberg, C. P. 2011. MorphoJ: an integrated software package for geometric morphometrics. *Molecular Ecology Resources* **11:** 353-357

Lesciotto, K. M., & Richtsmeier, J. T. (2019). Craniofacial skeletal response to encephalization: How do we know what we think we know?. *American journal of physical anthropology*, *168*, 27-46.

Levine, R. A., Garza, J. R., Wang, P. T., Hurst, C. L., & Dev, V. R. (2003). Adult facial growth: applications to aesthetic surgery. Aesthetic plastic surgery, 27(4), 265-268.

Levine, R. A. (2008). Aging of the midface bony elements. Plastic and reconstructive surgery, 121(1), 337-338.

Lieberman, D. E., & McCarthy, R. C. (1999). The ontogeny of cranial base angulation in humans and chimpanzees and its implications for reconstructing pharyngeal dimensions. *Journal of Human Evolution*, *36*(5), 487-517.

Mendelson, B., & Wong, C. H. (2012). Changes in the facial skeleton with aging: implications and clinical applications in facial rejuvenation. Aesthetic plastic surgery, 36(4), 753-760.

Milella, M., Franklin, D., Belcastro, M. G., & Cardini, A. Sexual differences in human cranial morphology: is one sex more variable or one region more dimorphic?. The Anatomical Record. DOI: 10.1002/ar.24626

Mitteroecker, P., & Bookstein, F. (2008). The evolutionary role of modularity and integration in the hominoid cranium. *Evolution: International Journal of Organic Evolution*, *62*(4), 943-958.

McHenry, H. M. (1994). Tempo and mode in human evolution. *Proceedings of the National Academy of Sciences*, *91*(15), 6780-6786.

Neubauer, S., Gunz, P., & Hublin, J. J. (2009). The pattern of endocranial ontogenetic shape changes in humans. *Journal of anatomy*, *215*(3), 240-255.

Pecora, N. G., Baccetti, T., & McNamara Jr, J. A. (2008). The aging craniofacial complex: a longitudinal cephalometric study from late adolescence to late adulthood. American journal of orthodontics and dentofacial orthopedics, 134(4), 496-505.

Roberts, N., Puddephat, M. J., & McNulty, V. (2000). The benefit of stereology for quantitative radiology. The British journal of radiology, 73(871), 679-697.

Rosenberg, K., & Trevathan, W. (2002). Birth, obstetrics and human evolution. *BJOG: An International Journal of Obstetrics & Gynaecology*, *109*(11), 1199-1206.

Rosas, A., & Bastir, M. (2002). Thin-plate spline analysis of allometry and sexual dimorphism in the human craniofacial complex. American Journal of Physical Anthropology: The Official Publication of the American Association of Physical Anthropologists, 117(3), 236-245.

Ross, C. F., & Ravosa, M. J. (1993). Basicranial flexion, relative brain size, and facial kyphosis in nonhuman primates. *American Journal of Physical Anthropology*, *91*(3), 305-324.

Sacher, G. A. (1959). Relation of lifespan to brain weight and body weight in mammals. In *Ciba Foundation colloquia on aging* (Vol. 5, pp. 115-133). Churchill London.

Smith, R. J., & Cheverud, J. M. (2002). Scaling of sexual dimorphism in body mass: a phylogenetic analysis of Rensch's rule in primates. International Journal of Primatology, 23(5), 1095-1135.

Smith, O. A., Duncan, C., Pears, N., Profico, A., & O'Higgins, P. (2021a). Growing old–do women and men age differently?. The Anatomical Record. DOI: 10.1002/ar.24584.

Smith, O. A., Nashed, Y. S., Duncan, C., Pears, N., Profico, A., & O'Higgins, P. (2020). 3D Modelling of Craniofacial Ontogeny and Sexual Dimorphism in Children. The Anatomical Record. DOI: 10.1002/ar.24582

Smith, T. D., Reynolds, R. L., Mano, N., Wood, B. J., Oladipupo, L., Hughes, G. K., & DeLeon, V. B. (2021b). Cranial synchondroses of primates at birth. The Anatomical Record. 04(5), 1020-1053.

Sowell, E. R., Thompson, P. M., Tessner, K. D., & Toga, A. W. (2001). Mapping continued brain growth and gray matter density reduction in dorsal frontal cortex: Inverse relationships during postadolescent brain maturation. *Journal of Neuroscience*, *21*(22), 8819-8829.

Thilander, B., & Ingervall, B. (1973). The human spheno-occipital synchondrosis II. A histological and microradiolic study of its growth. Acta Odontologica Scandinavica, 31(5), 323-336.

Ursi, W. J., Trotman, C. A., McNamara Jr, J. A., & Behrents, R. G. (1993). Sexual dimorphism in normal craniofacial growth. The Angle Orthodontist, 63(1), 47-56.

Whitford, T. J., Rennie, C. J., Grieve, S. M., Clark, C. R., Gordon, E., & Williams, L. M. (2007). Brain maturation in adolescence: concurrent changes in neuroanatomy and neurophysiology. *Human brain mapping*, *28*(3), 228-237.

Windhager, S., Mitteroecker, P., Rupić, I., Lauc, T., Polašek, O., & Schaefer, K. (2019). Facial aging trajectories: A common shape pattern in male and female faces is disrupted after menopause. *American journal of physical anthropology*, *169*(4), 678-688.

Yaggi, H. K., Concato, J., Kernan, W. N., Lichtman, J. H., Brass, L. M., & Mohsenin, V. (2005). Obstructive sleep apnea as a risk factor for stroke and death. *New England Journal of Medicine*, *353*(19), 2034-2041.

Zollikofer, C. P., Bienvenu, T., & Ponce de León, M. S. (2017). Effects of cranial integration on hominid endocranial shape. *Journal of Anatomy*, *230*(1), 85-105.

Figure legends

Figure 1. Example T1 MR images, illustrating placement of landmarks, as well as landmark configurations and wireframes: a) midsagittal image of a neonate; b) half axial and coronal images of a 2 year old; c) offset half coronal images of a 5 year old female; d) half coronal and axial images of a 29 year old female; e) offset half axial images of a 74 year old male; f) wireframe illustrating measurements of cranial base angle (CBA) and angle of facial kyphosis (AFK); g) lateral view of cranial landmark configuration and wireframe; h) frontal view of cranial landmark configuration and wireframe; i) lateral view of brain landmark configuration and wireframe; j) dorsal view of brain landmark configuration and wireframe. Refer to Table 3 for landmark definitions. Not to scale.

Figure 2. Plots of variables against chronological age (years) with locally estimated scatterplot smoothing fits (blue line) and standard errors (grey margin). Datum points are coded for gender (green, male; beige, female; salmon, unknown). Variables: cube root of endocranial volume (mm), ECl ; cranial centroid size (mm), CS; base centroid size (mm), Bcs; face centroid size (mm), Fcs; cranial base angle (degs.), CBA; angle of facial kyphosis (degs.), AFK; index of base over face centroid size, Bfi (unitless); index of endocranial over base size (unitless), IREb; index of endocranial over face size (unitless), IREf; index of endocranial centroid size over cranial centroid size (unitless), IREc.

Figure 3. Color coded Spearman correlation matrices for comparisons across all bins and across adjacent bins. Size and color of each circle indicates the magnitude of the

coefficient and direction of correlation, respectively (refer to color scale; p>0.05, marked by an X). Rectangle marked in red highlights spatial-packing related correlations. Variables: chronological age, Age (years); cube root of endocranial volume (mm), ECl ; cranial centroid size (mm), CS; base centroid size (mm), Bcs; face centroid size (mm), Fcs; cranial base angle (degs.), CBA; angle of facial kyphosis (degs.), AFK; index of base over face centroid size, Bfi (unitless); index of endocranial over base size (unitless), IREb; index of endocranial over face size (unitless), IREf; index of endocranial centroid size over cranial centroid size (unitless), IREc.

Figure 4. Boxplots and Wilcoxon tests between means from adjacent bins. Datum points are coded for gender (refer to key: green, male; beige, female; salmon, unknown). Variables: chronological age, Age (years); cube root of endocranial volume (mm), ECl ; cranial centroid size (mm), CS; base centroid size (mm), Bcs; face centroid size (mm), Fcs; cranial base angle (degs.), CBA; angle of facial kyphosis (degs.), AFK; index of base over face centroid size, Bfi (unitless); index of endocranial over base size (unitless), IREb; index of endocranial over face size (unitless), IREf; index of endocranial centroid size over cranium centroid size (unitless), IREc. P-values for tests are indicated by: *, p<0.05; **, p<0.01; ***, p<0.001; blank, p>0.05.

Figure 5. Color coded Spearman correlation matrices for comparisons across the oldest age bins (26.9-79 years) separated by gender. Size and color of each circle indicate the size of the coefficient and direction of correlation, respectively (refer to color scale; p>0.05, marked by an X). Variables: chronological age, Age (years); cube root of endocranial volume (mm), ECl ; cranial centroid size (mm), CS; base centroid size (mm), Bcs; face centroid size (mm), Fcs; cranial base angle (degs.), CBA; angle of facial kyphosis (degs.), AFK; index of base over face centroid size, Bfi (unitless); index of endocranial over base size (unitless), IREb; index of endocranial over face size (unitless), IREf; index of endocranial centroid size over cranial centroid size (unitless), IREc.

Figure 6. Boxplots and Wilcoxon tests between age bin 9 (26.9-46.6yrs; light blue boxes) and age bin 10 (46.6-79yrs; cream boxes) with separate comparisons for male (n= 28 & 26) and female (n=29 & 32). Boxplots show the 25th , 50th & 75th percentiles with hinges for datum points within 1.5 times the percentile range. Wilcoxon tests were one sided, either less or greater than with reference to the boxplots. Variables: cube root of endocranial volume (mm), ECl ; cranial centroid size (mm), CS; base centroid size (mm), Bcs; face centroid size (mm), Fcs; cranial base angle (degs.), CBA; angle of facial kyphosis (degs.), AFK; index of base over face centroid size, Bfi (unitless); index of endocranial over base size (unitless), IREb; index of endocranial over face size (unitless), IREf; index of endocranial centroid size over cranial centroid size (unitless), IREc.

Figure 7. Regression plots of allometric shape variation with frontal and lateral wireframe profiles (refer to Figure 1): a) Bin 1&2 variations against age (9%); b) Bin 1&2 variations against Bfi (8%); c) Bin 9&10 variations against age (2%). Scale factors were 1, 0.3, & 60 respectively.

Figure 8. Lateral and frontal profile wireframes (refer to Figure 1) illustrating allometric cranial changes represented by discriminant functions: a) Bin 1 vs. 2; b) Bin 5 vs. 6; c) Bin 10 vs. 9; d) females vs. males (all ages). Scale factor is 2 in each case and the starting shape is blue and the target bin shape is in red.

Figure 9. Dorsal and lateral profile wireframes (refer to Figure 1) illustrating allometric brain changes represented by discriminant functions: a) Bin 1 vs. 2; b) Bin 6 vs. 7; c) Bin 10 vs. 9; d) females vs. males (all ages). Scale factor is 2 in each case and the starting shape is blue and the target bin shape is in red.

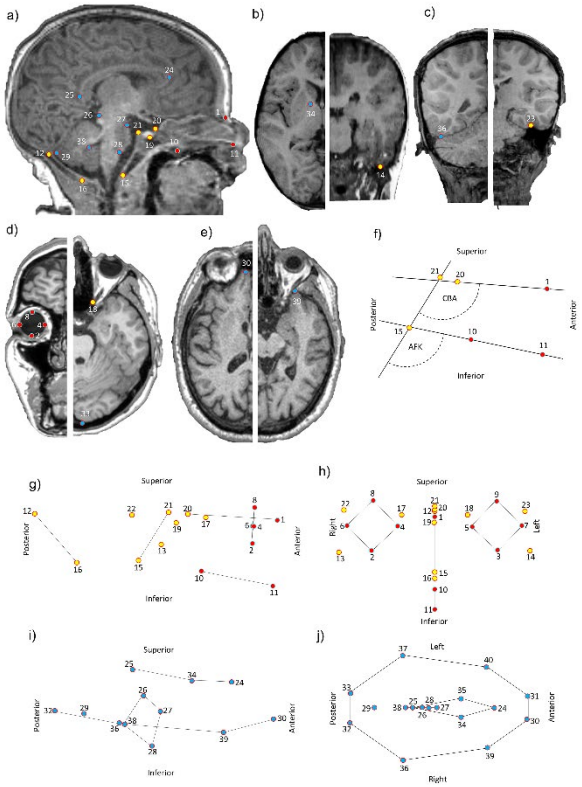

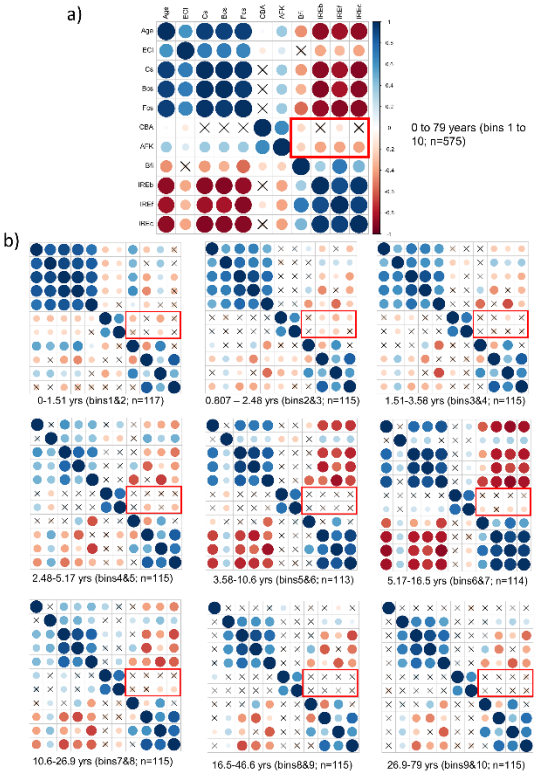

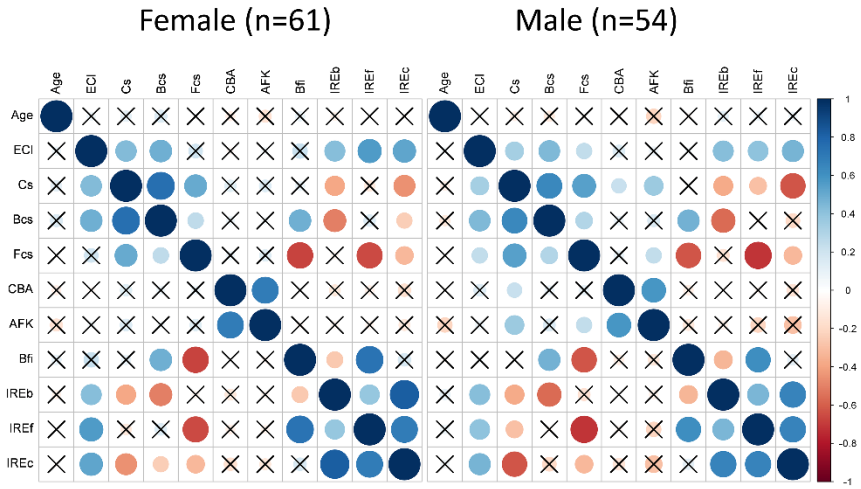

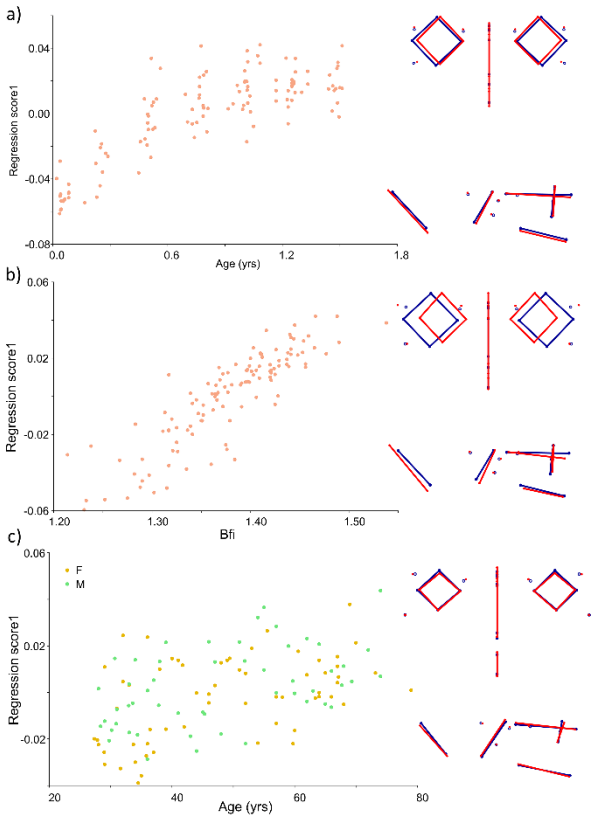

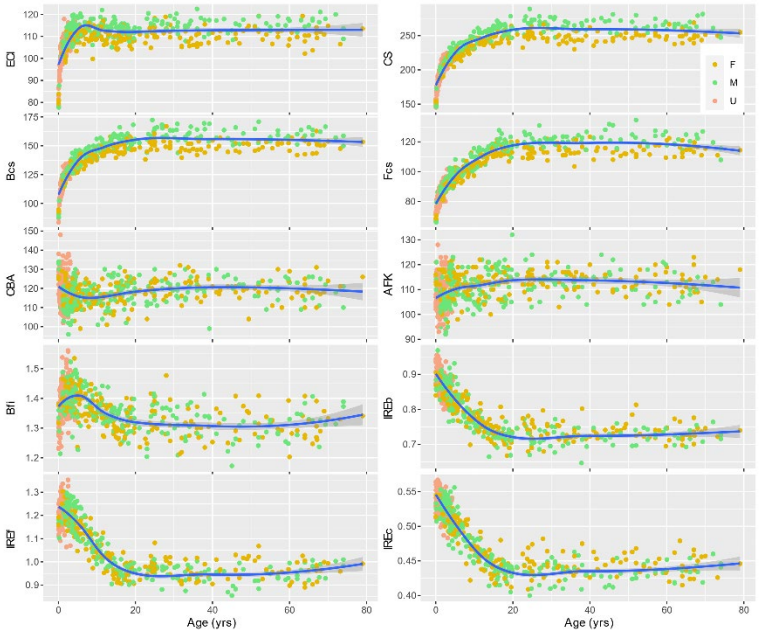

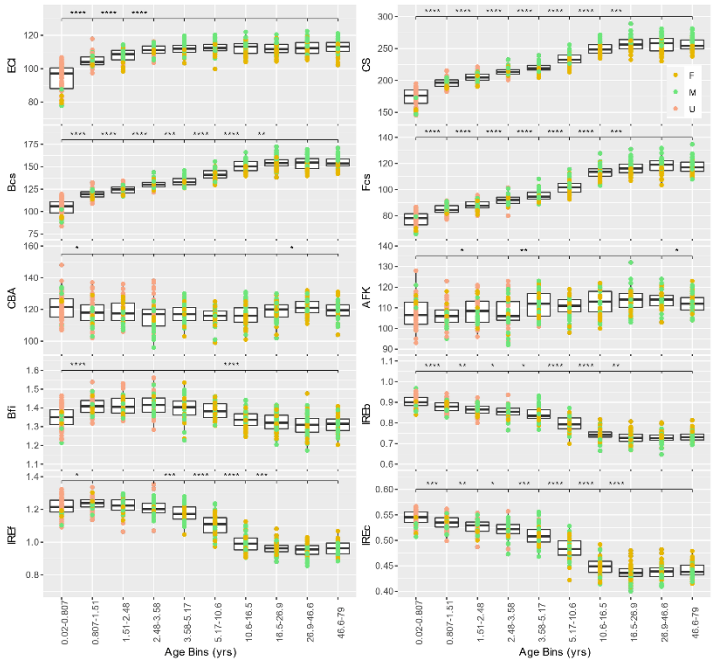

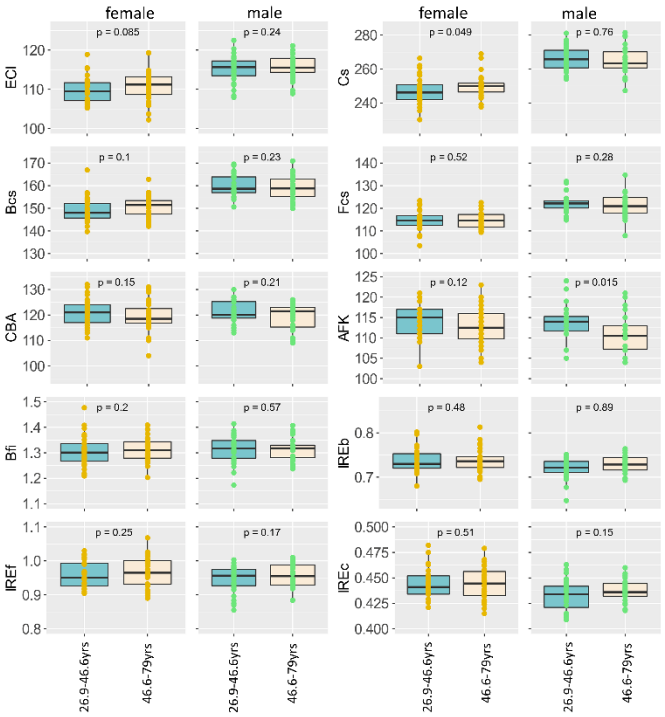

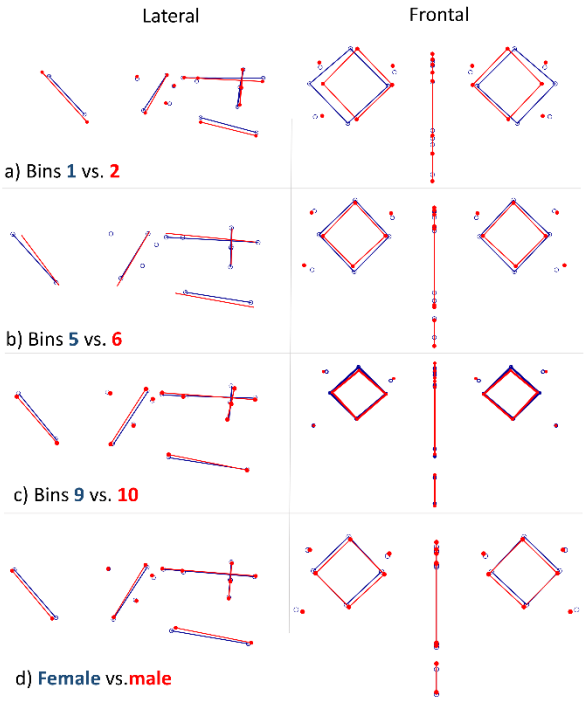

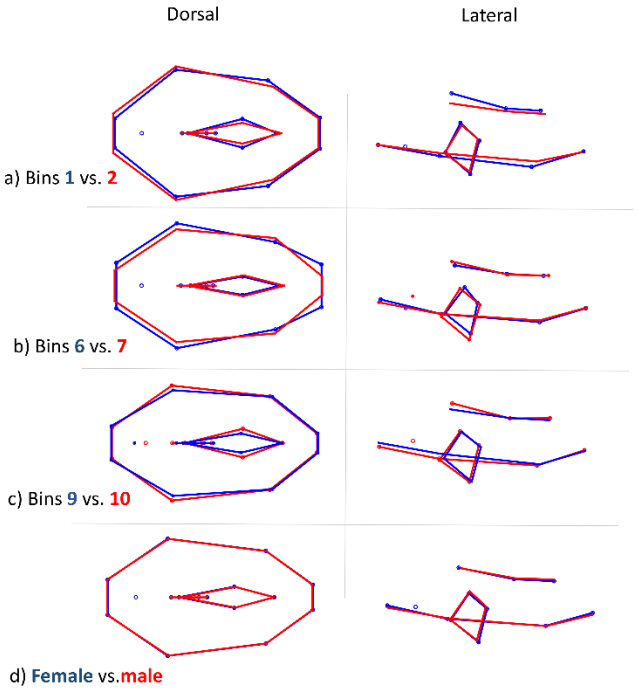

Table 1. Details for the MRI data repositories sampled.

Name	Age range	N sampled	MR sequence	Voxel Resolution (mm)	Links[2] & References
Information eXtraction from Images (IXI) project	20-79	142 (66M; 76F)	T1 & T2	1.07 x,y 1.20 – 1.25 z	http://brain-development.org/ixi-dataset/
Pediatric Imaging, Neurocognition, and Genetics (PING) Study[1]	3-20	192 (100M; 92F)	T1	1.00 - 1.07 x,y 1.25 z	https://nda.nih.gov/ Jernigan et al., 2016
NIMH Data Archive	0-5	241 (50M; 21F; 170?)	T1 & T2	1.00 - 1.25 x,y 0.94-3.00 z	https://nda.nih.gov/ Evans, 2006

[1] Now part of the NIMH Data archive; [2] Links correct at the time of submission.

Table 2. Sample details for the chronological age bins, including number of subjects and of each gender (if known).

Bin No.	Age range (yrs)	N_{total}	$N_{?}$	N_{male}	N_{female}
1	0.02-0.807	58	51	4	3
2	0.807-1.51	59	45	10	4
3	1.51-2.48	56	36	13	7
4	2.48-3.58	59	30	21	8
5	3.58-5.17	56	8	29	19
6	5.17-10.6	57	0	26	31
7	10.6-16.5	57	0	30	27
8	16.5-26.9	58	0	29	29
9	26.9-46.6	57	0	28	29
10	46.6-79	58	0	26	32

Table 3. Summary of landmarks, landmark sets & measurements

Landmark No.	Landmark name	Anatomical Set
1	Nasion	Face
2	Inferior Globe Right	Face
3	Inferior Globe Left	Face
4	Medial Globe Right	Face
5	Medial Globe Left	Face
6	Lateral Globe Right	Face
7	Lateral Globe Left	Face
8	Superior Globe Right	Face
9	Superior Globe Left	Face
10	Posterior nasal spine	Face
11	Anterior nasal spine	Face
12	Internal occipital protuberance	Base
13	Temporomandibular joint right	Base
14	Temporomandibular joint left	Base
15	Basion	Base
16	Opisthion	Base
17	Optic Canal Right	Base
18	Optic Canal Left	Base
19	Sella Turcica	Base
20	Tuberculum Sellae	Base
21	Clivus (Dorsum Sellae)	Base
22	Superior Petrous Ridge Right	Base
23	Superior Petrous Ridge Left	Base
24	Genu (corpus callosum)	Brain
25	Splenium (corpus callosum)	Brain
26	Tectum of midbrain	Brain
27	Superior pons	Brain
28	Inferior pons	Brain
29	Posterior cerebellum	Brain
30	Frontal pole right	Brain
31	Frontal pole left	Brain

32	Occipital pole right	Brain
33	Occipital pole left	Brain
34	Inflection of right internal capsule	Brain
35	Inflection of left internal capsule	Brain
36	Apex of right transverse cerebral fissure	Brain
37	Apex of left transverse cerebral fissure	Brain
38	Apex of median dorsal recess of 4^{th} ventricle	Brain
39	Temporal pole right	Brain
40	Temporal pole left	Brain
CBA	Cranial Base Angle	Anteroventral angle 1-20>15-21
AFK	Angle of Facial Kyphosis	Anteroventral angle 11-10>15-21
ECl	Cube root endocranial volume	$\sqrt[3]{\sum}$ endocranial voxels
Cs	Cranial centroid size	$\sqrt{\sum}$squared distances 1-23
Bcs	Basicranial centroid size	$\sqrt{\sum}$squared distances 12-23
Fcs	Facial centroid size	$\sqrt{\sum}$squared distances 1-11
Bfi	Ratio of basicranial over facial centroid size	Bcs/Fcs
IREb	Index of encephalization relative to basicranial centroid size	ECl/Bcs
IREf	Index of encephalization relative to facial centroid size	ECl/Fcs
IREc	Index of encephalization relative to cranial centroid size	ECl/Cs

Table 4. Wilcoxon tests for sexual dimorphism within age bins with 20 or more subjects per gender

Bin	N (f,m)	ECl	CS	Bcs	Fcs	CBA	AFK	Bfi	IREb	IREf	IREc
Bin 6	31,26	0.002	<0.001	<0.001	0.080	0.768	0.183	0.255	0.515	0.869	0.321
Bin 7	27,30	<0.001	<0.001	<0.001	0.030	0.159	0.654	0.005	0.195	0.409	0.798
Bin 8	29,29	<0.001	<0.001	<0.001	<0.001	0.707	0.741	0.738	0.093	0.140	0.010
Bin 9	29,28	<0.001	<0.001	<0.001	<0.001	0.832	0.676	0.605	0.014	0.106	0.004
Bin 10	32,26	<0.001	<0.001	<0.001	<0.001	0.873	0.154	0.957	0.166	0.264	0.051

Refer to Table 2 for bin age distributions. N sample sizes for females (f) & males (m); Variables: cube root of endocranial volume (mm), ECl ; cranial centroid size (mm), CS; base centroid size (mm), Bcs; face centroid size (mm), Fcs; cranial base angle (degs.), CBA; angle of facial kyphosis (degs.), AFK; index of basicranial over facial centroid size, Bfi (unitless); index of endocranial volume over base size (unitless), IREb; index of endocranial volume over face size (unitless), IREf; index of endocranial volume over cranial centroid size (unitless), IREc. Cell colors: light green, $p<0.001$; dark green, $p<0.05$; salmon, $p>0.05$.

Table 5 Percentage total allometric and non-allometric cranial shape variation predicted by each covariate using multivariate regression.

Group	**N**	**Cs**	**Age**	**Bfi**	**IREb**	**IREf**	**IREc**
All	575	25	19 (3)	13 (9)	25 (1)	27 (4)	26 (1)
Female	189	16	12 (3)	14 (7)	14 (<1)	18 (3)	15 (<1)
Male	216	19	15 (2)	14 (6)	19 (<1)	22 (2)	20 (<1)
Bin 1&2	117	9	9 (<1)	8 (4)	3 (4)	7 (4)	1 (2)
Bin 2&3	115	2	2	4	3	4	1
Bin 3&4	115	2	3	5	3	4	1
Bin 4&5	115	3	4	7	4	4	3
Bin 5&6	113	5	8	8	5	8	5
Bin 6&7	114	5	9	10	6	10	7
Bin 7&8	115	3	4	6	2	4	3
Bin 8&9	115	4	3	7	3	3	3
Bin 9&10	115	3	2	7	2	4	3

Based on separate Procrustes fits; computed with symmetric component shape variables as the dependents and one covariate as the independent (10,000 permutations); non-allometric regressions computed if comparisons against centroid size (Cs) predict >5% of the shape variation (non-allometric values given in brackets). Variables: cranial centroid size, Cs (mm); chronological age, Age (years); index of basicranial over facial centroid size, Bfi (unitless); index of endocranial volume over base size (unitless), IREb; index of endocranial volume over face size (unitless), IREf; index of endocranial volume over cranial centroid size (unitless), IREc. Refer to Table 2 Bin age ranges. Cell colors: light green, $p<0.001$; dark green, $p<0.05$; salmon, $p>0.05$.

Table 6. Discrimination functions for gender and age bins across allometric and non-allometric shape spaces representing the cranium and brain.

		Cranium				Brain			
		Allometric		Non-allometric		Allometric		Non-allometric	
Comparison	N	PD	P-value	PD	P-value	PD	P-value	PD	P-value
f-m	189,216	0.0157	<0.001	0.0208	<0.001	0.0136	<0.001	0.0189	<0.001
1-2	58,59	0.0329	<0.001	0.0426	<0.001	0.0386	<0.001	0.0385	<0.001
2-3	59,56	0.0173	0.024	0.0135	0.261	0.0138	0.1950	0.0135	0.215
3-4	56,59	0.0192	0.002	0.0140	0.189	0.0167	0.019	0.0109	0.610
4-5	59,56	0.0220	<0.001	0.0154	0.034	0.0233	<0.001	0.0195	0.004
5-6	56,57	0.0297	<0.001	0.0185	<0.001	0.0249	<0.001	0.0195	0.002
6-7	57,57	0.0286	<0.001	0.0215	<0.001	0.0505	<0.001	0.0499	<0.001
7-8	57,58	0.0192	<0.001	0.0170	0.002	0.0309	<0.001	0.0284	<0.001
8-9	58,57	0.0242	<0.001	0.0248	<0.001	0.0311	<0.001	0.0300	<0.001
9-10	57,58	0.0161	0.010	0.0161	0.023	0.0396	<0.001	0.0387	<0.001

PD, Procrustes Distance; *, 1000 permutations; same fit for all bins; f, female; m, male; refer to Table 2 for ages; cell colors: light green, p<0.001; dark green, p<0.05; salmon, p>0.05.

Table 7. Statistics for tests of integration and modularity between the cranium (C), brain (Br), basicranium (Ba) and face (F).

Group	**N**	**Partial Least Squares[1]**		**Modularity Test[2]**		**Covariance Ratios[3]**			
		RV Br-C	RV F-Ba	% Br-C	% F-Ba	CR Br-C	Z_{CR} Br-C	CR F-Ba	Z_{CR} F-Ba
All	575	0.71	0.62	2	22	0.94	-2.48	0.96	-1.94
Females	189	0.61	0.43	3	10	0.83	-2.44	0.88	-2.57
Males	216	0.74	0.52	78	25	0.95	-2.04	0.93	-1.80
Bin 1&2	117	0.46	0.25	24	<1	0.80	-3.01	0.65	-4.40
Bin 2&3	115	0.41	0.32	3	<1	0.78	-3.07	0.76	-2.96
Bin 3&4	115	0.36	0.28	4	2	0.74	-3.52	0.72	-2.86
Bin 4&5	115	0.31	0.29	<1	1	0.69	-3.77	0.74	-2.67
Bin 5&6	113	0.36	0.31	4	3	0.73	-2.84	0.78	-2.48
Bin 6&7	114	0.58	0.29	52	3	0.88	-1.94	0.71	-3.15
Bin 7&8	115	0.42	0.26	59	2	0.79	-2.35	0.68	-2.93
Bin 8&9	115	0.36	0.28	19	6	0.73	-2.96	0.69	-2.30
Bin 9&10	115	0.33	0.28	9	5	0.73	-2.91	0.68	-2.74

[1]Coefficients of association (RV) computed in MorphoJ between two sets of landmarks based on PLS within configurations with 250 randomization trials yielding p<0.001 for all coefficients; [2] 10,000 random contiguous partitions with percentages of random partitions with lower RV scores than the hypothetical models (Br-C, brain-cranium module; F-Ba, face-base module); [3] covariance ratio coefficients (CR) with p-values for <1 (modularity) and modularity effect size (Z_{CR}) computed in Geomorph with 1,000 permutations. Separate fits for each group. Cell colors: light green, p<0.001; dark green, p<0.05; salmon, p>0.05.